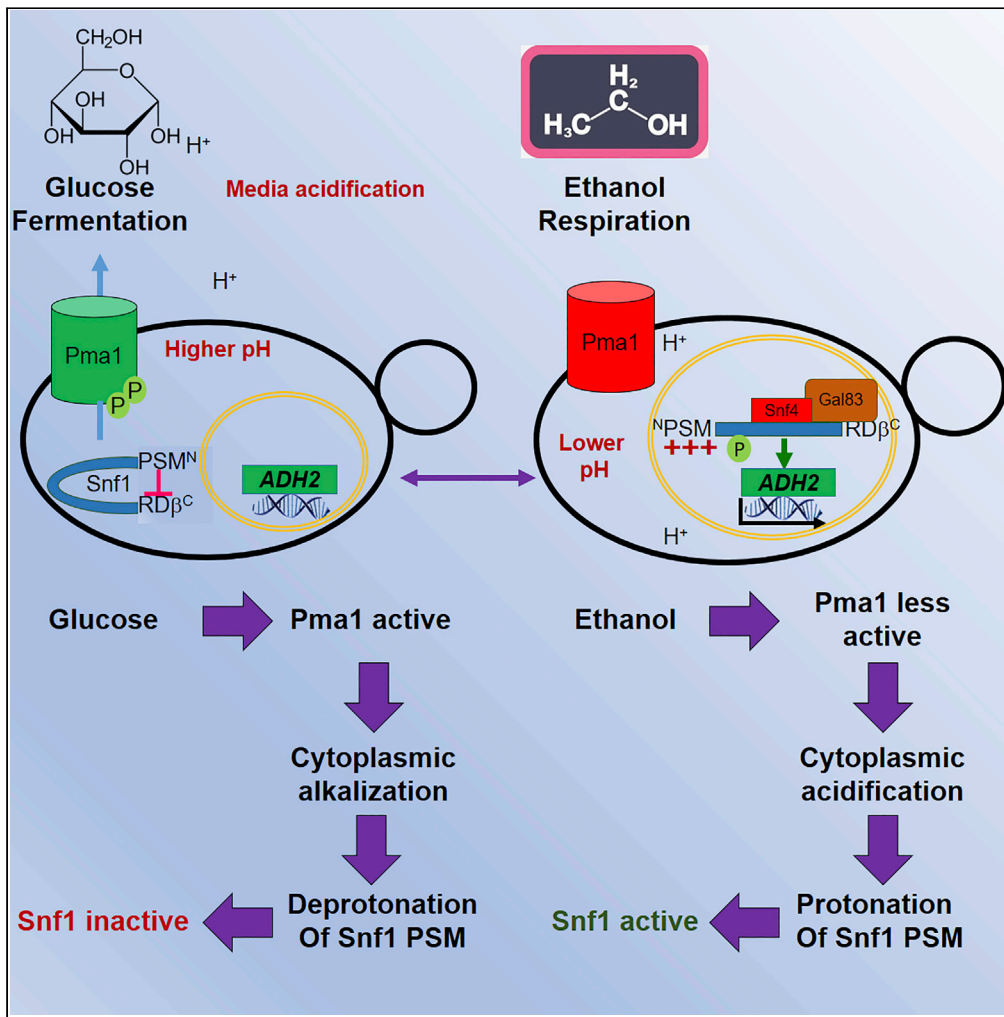


Article

Regulation of yeast Snf1 (AMPK) by a polyhistidine containing pH sensing module



Kobi J. Simpson-Lavy, Martin Kupiec

martin@tauex.tau.ac.il

Highlights

Glucose inhibits Snf1 by activating Pma1 to pump protons out of the cell

Increased cytoplasmic alkalinity deprotonates the N-terminal polyhistidines of Snf1

Deprotonated polyhistidines bind the Regulatory domain to inhibit Snf1

Number of histidines in this motif correlates to Snf1 activity.

Simpson-Lavy & Kupiec, iScience 25, 105083 October 21, 2022 © 2022 The Authors. <https://doi.org/10.1016/j.isci.2022.105083>



Article

Regulation of yeast Snf1 (AMPK) by a polyhistidine containing pH sensing module

Kobi J. Simpson-Lavy¹ and Martin Kupiec^{1,2,*}

SUMMARY

Cellular regulation of pH is crucial for internal biological processes and for the import and export of ions and nutrients. In the yeast *Saccharomyces cerevisiae*, the major proton pump (Pma1) is regulated by glucose. Glucose is also an inhibitor of the energy sensor Snf1/AMPK, which is conserved in all eukaryotes. Here, we demonstrate that a poly-histidine (polyHIS) tract in the pre-kinase region (PKR) of Snf1 functions as a pH-sensing module (PSM) and regulates Snf1 activity. This regulation is independent from, and unaffected by, phosphorylation at T210, the major regulatory control of Snf1, but is controlled by the Pma1 plasma-membrane proton pump. By examining the PKR from additional yeast species, and by varying the number of histidines in the PKR, we determined that the polyHIS functions progressively. This regulation mechanism links the activity of a key enzyme with the metabolic status of the cell at any given moment.

INTRODUCTION

pH homeostasis is vital for cellular processes and life. Whereas vertebrates regulate both intracellular and plasma pH with a bicarbonate/carbon dioxide buffer system (Burggren and Bautista, 2019), plants (Cosse and Seidel, 2021) and fungi utilize proton pumps to export protons from the cytoplasm into the vacuole and extracellular medium (Kane, 2016). Cytoplasmic pH regulates many processes, such as glycolysis (van Leemputte et al., 2020), membrane biogenesis (Young et al., 2010), storage of metabolic enzymes as filaments (Petrovska et al., 2014) and even solidification of the cytoplasm with a concomitant reduction of macromolecular diffusion (Munder et al., 2016) and in metazoans, apoptosis (Lagadic-Gossmann et al., 2004). The proton gradient established is used to drive transport of nutrients and minerals such as monovalent cations (Ariño et al., 2019), amino acids (Saliba et al., 2018), glycerol (Ferreira et al., 2005), hexoses (Lagunas, 1993) and nucleosides (Loewen et al., 2003).

Yeasts maintain an internal pH of 7.2 during growth on glucose by the pumping of protons from the cytoplasm across the plasma membrane by the Pma1 pump (which is the most abundant plasma membrane protein and the highest consumer of ATP in *S. cerevisiae* (Serrano et al., 1986; Zhao et al., 2021)), and into the vacuole by Vma1. On glucose starvation, these pumps are inactivated, leading to a rapid acidification of the cytoplasm to pH 5.7 (Martínez-Muñoz and Kane, 2008; Orij et al., 2009; Dechant et al., 2010). Glucose causes a slow increase in expression of Pma1 (Rao et al., 1993; García-Arranz et al., 1994) and activates its phosphorylation at S899 (increasing affinity of Pma1 for ATP) and at S911/T912 (increasing V_{max} of Pma1) (Goossens et al., 2000; Eraso et al., 2006). Altogether, addition of glucose causes an increase in Pma1 activity by up to ten-fold. Trafficking of Pma1 to the plasma membrane involves Exp1 and Psg1. In the absence of Exp1, Pma1 is retained in the endoplasmic reticulum, whereas deletion of *PSG1* increases Pma1 degradation in the vacuole (Geva et al., 2017). On glucose deprivation the phosphorylation of Pma1 at S899 is reversed by the Glc7 phosphatase (Mazón et al., 2015). Glucose deprivation also induces Hsp30 expression (Hahn and Thiele, 2004) to inhibit Pma1 activity (Panaretou and Piper, 1992; Piper et al., 1997).

The switch from fermentation of hexoses (such as glucose or fructose) to produce ethanol, to the respiration of poor carbon sources (glycerol, ethanol, etc.) is promoted by the Snf1 kinase (AMP-activated Protein Kinase or AMPK in metazoans) (Ghillebert et al., 2011). Snf1 induces expression of genes involved in the respiration of alternative carbon sources and gluconeogenesis by activating transcription factors such as Adr1 (e.g., to express *ADH2*, which is used as a reporter for Snf1 activity in this study) (Ratnakumar et al., 2009) and Cat8 (e.g., to express *FBP1*, *PCK1*) (Charbon et al., 2004), and by inhibiting repressors such as

¹The Shmunis School of Biomedicine & Cancer Research, Tel Aviv University, Ramat Aviv 69978, Israel

²Lead contact

*Correspondence:

martin@tauex.tau.ac.il

<https://doi.org/10.1016/j.isci.2022.105083>



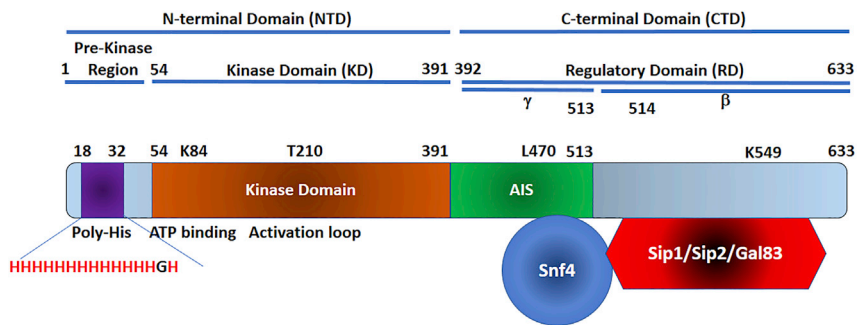


Figure 1. Schematic Diagram of *S. cerevisiae* Snf1

Schematic diagram showing domains and regions of Snf1, with important residues and motifs. Aa1-53 is referred to as the pre-kinase region (PKR) containing a polyHIS tract at Aa18-32. Aa54-391 comprises the kinase domain (KD) – mutation of K84R prevents ATP-binding (kinase dead) and the activation loop phosphorylation site is at T210. Together the PKR and KD comprise the N-terminal domain (NTD). The regulatory domain (RD) comprises aa392-633 and comprises the entire C-terminal domain (CTD); The γ -subunit Snf4 binds to the auto-inhibitory sequence (AIS) (RD- γ) to prevent it from inhibiting the kinase domain – mutation of L470 inactivates the auto-inhibitory sequence. The β -subunits Sip1, Sip2 or Gal83 bind the far C-terminus (RD- β). K549 is SUMOylated in the presence of glucose and the SUMO interacts with the kinase domain.

Mig1 and Nrg1 [to express *SUC2*, *GAL1* (Treitel et al., 1998; Zhou and Winston, 2001)]. In addition to regulating transcription, Snf1 also phosphorylates metabolic enzymes such as Acc1 (as a downregulation mechanism) (Woods et al., 1994), and the arrestins Rod1 and Rog3 to regulate the stability of plasma membrane carbon transporters (Llopis-Torregrosa et al., 2016).

When glucose is not present, Snf1 is activated by phosphorylation at T210 (Hong et al., 2003); this site is dephosphorylated on addition of glucose (Ruiz et al., 2013). Snf1 activity is also downregulated by SUMOylation at lysine 549 in response to glucose (Simpson-Lavy and Johnston, 2013). In the absence of glucose, Snf1 associates with a gamma-protein activator (Snf4), and one of three beta-localizing proteins (Sip1, Sip2, and Gal83) (Elbing et al., 2006); this association increases Snf1 localization at the vacuolar membrane, plasma membrane and nucleus respectively. Snf1 localization to the nucleus by Gal83 is inhibited by glucose (Vincent et al., 2001).

The Snf1 protein can be divided into an N-terminal domain (NTD) and a C-terminal domain (CTD, also called regulatory domain-RD). The NTD is composed of a pre-kinase domain (PKR – amino acids 1-53) and a kinase domain (KD, aa 54-391) (Figure 1). In the presence of glucose, the regulatory domain interacts with, and inhibits, the kinase domain. On phosphorylation of Snf1 at T210, Snf4 prevents the association of the kinase and regulatory domain by interacting with aa 460-498 of Snf1, preventing the auto-inhibition of Snf1 activity (Jiang and Carlson, 1996) (Amodeo et al., 2007); thus the region between amino acids 392-513 is referred to as RD- γ . The beta proteins (Sip1, Sip2, and Gal83) interact with aa 515-633 of Snf1 (Jiang and Carlson, 1997) (this region is thus referred to as RD- β). Snf1 must associate with Snf4 and one of the beta proteins for a stable, active complex to form (Elbing et al., 2006). Whereas the kinase domain is conserved across species, the PKR (aa1-53) shows sequence diversity. This region of the yeast protein contains an unusual polyHIS motif, comprising 13 histidines followed by a glycine and one more histidine (Celenza and Carlson, 1989) (Figure 1). In this work, we demonstrate that the polyHIS motif in the PKR acts as a progressive pH-sensing module (PSM) that controls Snf1 activity by histidine protonation/deprotonation as a consequence of, and in response to, glucose deprivation. This regulatory mechanism controls Snf1 activity independently from phosphorylation at T210, by modulating both internal interactions within Snf1 and between Snf1 and the β -subunits Gal83, Sip1, and Sip2.

RESULTS

The polyHIS tract of Snf1 regulates SNF1 activity

Whereas the kinase domain of Snf1 (aa54-391) shows remarkable conservation across fungi and indeed eukaryotes, the PKR (aa1-53) is heterogeneous (Figure S1). This region of the Snf1 of many *Saccharomyces*, *Candida*, and *Kluyveromyces* species, but not fission yeasts such as *Schizosaccharomyces pombe* or vertebrates, contains a polyhistidine tract of up to 13 consecutive residues which is highly conserved in the *Saccharomyces* species. This is the maximal number of consecutive histidines in any *S. cerevisiae* protein,

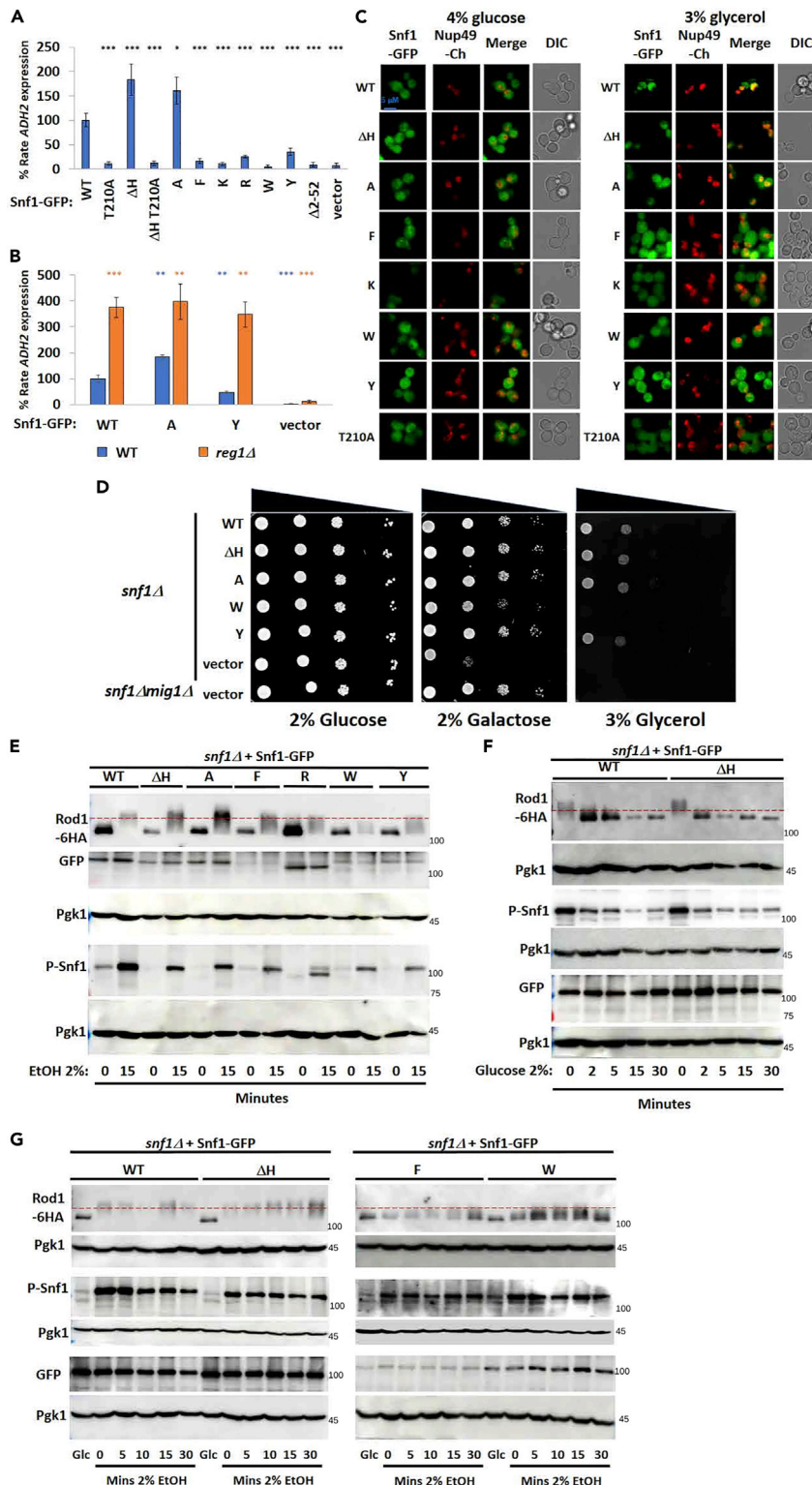


Figure 2. The polyHIS tract of Snf1 regulates ADH2 expression

(A and B) ADH2 expression in *snf1Δ* cells (and *snf1Δreg1Δ* cells (B)) expressing *prSNF1::Snf1-GFP* from plasmids with the indicated mutations [deletion of polyHIS (ΔH), substitution to poly^A (A), poly^F (F), poly^W (W), poly^Y (Y), T210A or empty vector]. N = 3. T-test was performed against WT cells (far left, blue). NS = not significant, * = p ≤ 0.05, ** = p ≤ 0.01, *** = p ≤ 0.001.

Figure 2. Continued

- (C) Localization of Snf1-GFP was determined as described in the [Star Methods](#) section. Quantification of these data is provided in [Figure S1](#).
- (D) Growth of *snf1Δ* cells with different mutations of the polyHIS tract in the PKR on different carbon sources. The *snf1Δ* cells do not grow on galactose or glycerol medium, and *snf1Δmig1Δ* cells grow on galactose but not glycerol medium.
- (E) Rod1-6HA and Snf1 T210 phosphorylation following transfer from 4% glucose medium to 2% ethanol medium for 15 min. Cells were grown and processed as described in materials and methods. Molecular weight markers are indicated to the right of the image in kDa.
- (F) Rod1-6HA and Snf1 T210 phosphorylation following addition of glucose to 2% in ethanol media grown cells. Cells were grown and processed as described in materials and methods. Molecular weight markers are indicated to the right of the image in kDa.
- (G) Phosphorylation of Rod1-6HA and Snf1 T210 following transfer from 4% glucose to 2% ethanol media. Cells were grown and processed as described in materials and methods. The red dotted line indicates maximal phosphorylation of Rod1. The two images (for WT/ΔH and F/W cells) were aligned using the protein ladder (visible on the left of each image). Molecular weight markers are indicated to the right of the image in kDa.

and indeed only 12 other proteins of the *S. cerevisiae* proteome contain more than 6 His (and thus all would be expected to be potential contaminants of a nickel pulldown). An early report into Snf1 structure and function declared that deletion of this tract had no negative effect on invertase activity ([Celenza and Carlson, 1989](#)), although no data were shown. Amino acids 2-52 (the PKR) is required for Snf1 function ([Figure 2A](#)). We deleted the 13 histidines, the next glycine and a fourteenth histidine (*snf1^{ΔH}*) and found that although there is no negative effect on Snf1 function, there is an increase in *ADH2* expression ([Figure 2A](#)). Lest this phenotype be because of the absence of amino acids (i.e., joining amino acid 17 to 33) we mutated all of the fourteen histidines to either alanine (A), lysine (K), arginine (R), phenylalanine (F), tryptophan (W) or tyrosine (Y). The rationale behind these changes is as follows: The imidazole ring of histidine is deprotonated at physiological pH (pKa = 6.5) but is protonated at lower pH values (acquiring a positive charge). Deprotonated histidine, as well as phenylalanine, tryptophan and tyrosine also engage in π -bond stacking ([Liao et al., 2013](#)). In contrast, the aromatic ring of phenylalanine cannot be protonated and thus at low pH lacks a positive charge. Tyrosine introduces a negative polarity (by the phenol group), whereas the indole group of tryptophan is aromatic, contains nitrogen but is neutral and bulkier than imidazole. Arginine and lysine were used to create a strongly positively charged motif, similar to protonated polyHIS. Substitution of the poly-histidine to poly-alanine results in the same phenotype as a deletion (elevated activity), whereas phenylalanine and tryptophan substitutions eliminate, and tyrosine substitution lowers, Snf1 function ([Figure 2A](#)). Surprisingly, poly-lysine and poly-arginine mutations also eliminated Snf1 activity. Because Snf1 regulates the transcription of many genes, we examined the expression of *ACS1* ([Figure S2A](#)) and *JEN1* ([Figure S2B](#)) and obtained similar results to *ADH2* ([Figure 2A](#)). We then asked whether the increased Snf1 function of the *snf1^{ΔH}* mutation renders Snf1 activity independent from phosphorylation at T210. A double *snf1ΔH, T210A* mutant, however, does not permit expression of *ADH2* ([Figure 2A](#)); therefore, even in the absence of the polyHIS tract, phosphorylation at T210 is required for Snf1 function. Because the tyrosine mutant still retains about 30% Snf1 activity, we wondered whether hyperphosphorylation of T210 by deletion of *Reg1* ([Sanz et al., 2000](#)) could suppress this phenotype. Indeed, deletion of *reg1* enhances Snf1 activity to the same extent whether wild-type, alanine (A) or tyrosine (Y) mutant ([Figure 2B](#)).

In the presence of glucose, Snf1 is cytoplasmic. Snf1 localization to the nucleus, vacuole, and cytoplasm in the absence of glucose is regulated by the beta-subunits Gal83, Sip1 and Sip2 respectively ([Vincent et al., 2001](#)). We found the distribution of Snf1^{ΔH} and Snf1^A to be similar to that of the wild-type both in the presence and absence of glucose ([Figures 2C and S2C](#)). However, Snf1^R, Snf1^F, Snf1^W and Snf1^{T210A} are excluded from the nucleus in the absence of glucose, with Snf1^Y exhibiting an intermediate phenotype. This suggests that, as phosphorylation of T210, the N-terminal PKR affects the interaction of the far-C-terminal of Snf1 with Gal83. Snf1^Y does not exhibit a growth defect on glycerol or galactose media, whereas Snf1^W does not grow on glycerol yet only has a slight growth defect on galactose medium ([Figure 2D](#)).

The mutations of the polyHIS tract did not prevent phosphorylation at T210 following glucose withdrawal ([Figure 2E](#)); even when Snf1 protein levels were decreased compared to wild-type, T210 phosphorylation was normal. We noted that Snf1^R appears to undergo N-terminal truncation (the GFP is at the C-terminus) but is phosphorylated in ethanol media at T210 ([Figure 2E](#)) – this results in a phenotype similar to Snf1^{Δ2-52}. The mutations of the polyHIS tract did not prevent T210 phosphorylation following glucose withdrawal ([Figure 2E](#)).

Rod1 is an arrestin that targets substrates such as Jen1 (Fujita et al., 2018) for ubiquitylation by Rsp5. Rod1 is phosphorylated and inhibited by Snf1 (Beçuwe et al., 2012). Whereas Rod1 is maximally phosphorylated in Snf1^{WT}, Snf1^{ΔH} and Snf1^A cells, Rod1 is incompletely phosphorylated in cells with the aromatic mutations or the Snf1^R mutation (Figure 2E), further showing that Snf1 activity is compromised by these mutations.

We next performed a time-course for Snf1^{WT} and Snf1^{ΔH} inactivation. Close time points were used because we suspected that any differences might only be apparent during the first 15 min following glucose addition. On addition of glucose to ethanol grown cells, Snf1^{ΔH} is inactivated faster than Snf1^{WT} (as seen both by phosphorylation at T210 and Rod1 phosphorylation) (Figure 2F) which may be because of this mutant having less control mechanisms regulating its activity. On removal of glucose from media (and subsequent growth in 2% ethanol), Rod1 in both WT and Snf1^{ΔH} cells was already maximally phosphorylated just after the washes, whereas Rod1 was not maximally phosphorylated in Snf1^F or Snf1^W cells even after 30 min. However, phosphorylation of Snf1 at T210 was not affected by these mutations (Figure 2G).

The polyHIS tract regulates internal and external interactions of Snf1

We examined the interactions between Snf1 and the beta and gamma subunits of SNF1 by yeast two-hybrid. For comparison, and as verification of the constructs, we included the published interaction between the kinase domain (1-391) or the regulatory domain (392-633) of Snf1 (Jiang and Carlson, 1996) and the beta or gamma proteins. Snf4 interacts with the RD γ (aa460-498) region of Snf1 (Jiang and Carlson, 1996; Amodeo et al., 2007), far away from the histidine tract (Figure 1). The interaction between Snf1 and Snf4 is unaffected by changes in the polyHIS tract (Figure 3A). In contrast, deletion (Δ H) or substitution to alanine (A) of the polyHIS tract enhances the interaction between Snf1 and Gal83 (Figure 3B) which interacts with RD β at aa515-633 (Jiang and Carlson, 1997). Substitution to tyrosine (Y) lowers the interaction, and conversion of the histidines to phenylalanine (F), tryptophan (W) or arginine (R), abolishes the Snf1/Gal83 interaction altogether, similarly to the T210A mutation. Interactions of Snf1 with the other beta subunits, Sip1 (Figure S3A) or Sip2 (Figure S3B) were not enhanced by deletion of the polyHIS tract (Δ H) or its mutation to alanine (A) but interaction of Snf1 with Sip1 or Sip2 was lowered to levels seen in the T210A mutant when the polyHIS was substituted with arginine, phenylalanine, tryptophan or tyrosine. Because histidine is more deprotonated in glucose medium (because of high Pma1 pumping of protons into the extracellular medium), it seems that the neutral aromatic amino acids phenylalanine and tryptophan (and to lesser extent tyrosine) mimic the deprotonated, neutral form of histidine.

How can mutations at the far N-terminus of Snf1 affect interactions in the C-terminal domain? One possibility is that the polyHIS tract is involved in the intramolecular interaction of the NTD and CTD (Jiang and Carlson, 1996). Indeed, deletion (Δ H) or substitution to alanine (A) decreases this inhibitory interaction even in glucose and severely in ethanol medium, whereas interaction between the NTD and CTD remains high in ethanol when the polyHIS tract is substituted with phenylalanine, tyrosine or tryptophan. Substitution to arginine (R) results in the lowest interaction between the NTD and CTD, possibly because of the strong positive charge in the PKR of the NTD (Figure 3C). Because SUMOylation at K549 within RD- β has been found to be involved in the inhibition of Snf1 by interaction with SUMO-Interacting-Motifs at I129 in the kinase domain (Simpson-Lavy and Johnston, 2013), we examined the effects of a K549R mutation in the regulatory domain on the interaction with the kinase domain. SUMOylation at K549 is a prerequisite for interaction between the kinase and regulatory domains in glucose media, even when the polyHIS is substituted to aromatic amino acid. (Figure S3C). Therefore, regulation of Snf1 by SUMOylation is independent from regulation of Snf1 through the polyHIS motif in the PKR. Together, these data suggest that the polyHIS tract is a regulator of the kinase/regulatory domain interaction at the β -subunit binding site, thereby controlling accessibility of β -subunits and thus Snf1 localization and activity.

We next examined interactions of the PKR (1-53) with the kinase domain (KD) (54-391) and the regulatory domain (CTD) (392-633) of Snf1. In glucose medium, the PKR interacts with the regulatory domain. This interaction is mediated via the C-terminal half of the regulatory domain (aa514-633) that contains the binding sites of the β -subunits (RD- β); and is absent in ethanol-based medium. Whereas interaction of the NTD with the CTD is SUMO dependent, interaction of the PKR with either the whole CTD or RD β is SUMO-independent (i.e., not affected by K549R) (Figure 3D). The PKR contacts the kinase domain in the absence of glucose (Figure 3D). Because this suggests that the PKR interacts with different areas of Snf1 depending on the glucose status of the environment, we determined the requirements for this interaction. This interaction requires histidine or arginine: deletion or substitution to alanine or the aromatic amino acids all prevent

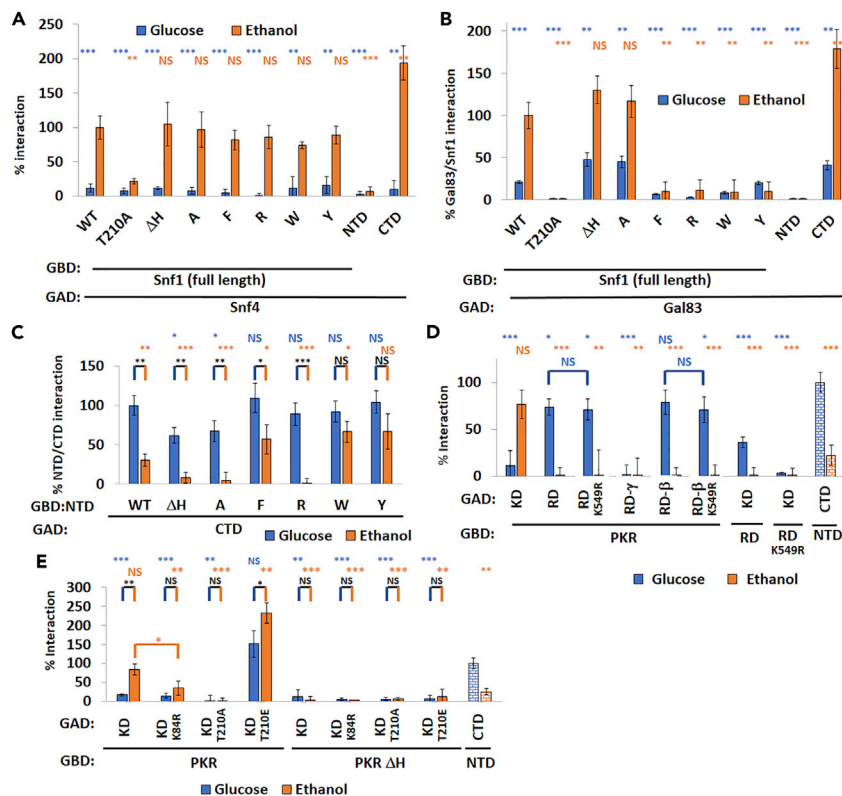


Figure 3. The polyHIS tract regulates Snf1 interactions

(A) Yeast two-hybrid experiment showing interaction of Snf4 with indicated Snf1 polyHIS mutants in glucose and ethanol media. N = 3.

(B) As A. but with pGAD-Gal83 in lieu of pGAD-Snf4. N = 3.

(C) As A. but with pGAD-Snf1^{392–633} (CTD) and pGBD-Snf1^{1–391} (NTD) with indicated mutations [deletion of polyHIS (ΔH), substitution to poly^A (A), poly^F (F), poly^W (W), poly^Y (Y), T210A]. N = 3. T-tests were conducted against WT ethanol (far left, orange) for A and B, and against WT glucose (far left blue) for C. NS = not significant, * = p ≤ 0.05, ** = p ≤ 0.01, *** = p ≤ 0.001.

(D and E) As (C) but with indicated pGBD and pGAD Snf1 fragments. PKR = amino acids 1-53, KD = 54-391, NTD = 1-391, RD/CTD = 392-633, RD-α = 392-513, RD-β = 514-633. N = 3. T-tests were conducted against NTD/CTD glucose (far right blue brick) for D and E. NS = not significant, * = p ≤ 0.05, ** = p ≤ 0.01, *** = p ≤ 0.001.

this interaction from occurring, whereas substitution to arginine results in some interaction between the PKR and KD (Figure S3D). This may be because of the diffuse positive charge of the protonated imidazole ring. In addition to the polyHIS tract, this interaction also requires Snf1 kinase activity because the K84R mutation abolishes the interaction, and phosphorylation at T210. Indeed, this interaction is elevated (even in glucose-grown cells) when T210 is replaced with a phospho-mimicking glutamate (T210E, Figure 3E). These results suggest that one of the effects of phosphorylation at T210 may be to attract the PKR via the polyHIS tract, thereby unlocking the beta subunit binding site.

The polyHIS tract of Snf1 functions as a pH sensing module (PSM)

Because the interactions between the kinase and the regulatory domains mediated by the polyHIS tract are mimicked by substitution with neutral aromatic amino acids, and are high in glucose and low in ethanol, we considered how this could be regulated. One possibility is that respiration-derived reactive oxygen species (ROS) could oxidize histidine to produce 2-oxo-histidine as occurs in the PerR peroxide sensor in *B. subtilis* (Traoré et al., 2009) triggering its proteolysis (Ahn and Baker, 2016). Incubation of cells with the ROS scavenger N-acetyl cysteine does not affect Snf1 activity. Although treatment of cells with diamide does increase Snf1^H activity (Figure S4A), diamide treatment also further elevates Snf1^{ΔH} activity, and therefore the oxidative stress induced increase in Snf1 activity is polyHIS-independent.

Cytoplasmic alkalinization as a consequence of Pma1 pumping protons into the external media in response to glucose functions as a second messenger signal (Dechant et al., 2010). We therefore investigated whether mutations or drugs that affect Pma1 activity regulate Snf1 by modulating the charge of the histidines of the polyHIS tract. We increased Pma1 activity (glucose mimicking, resulting in cytoplasmic alkalinization) by two methods simultaneously. Truncation of the final 18 amino acids of Pma1 (*PMA1-Δ901*) increases Pma1 activity to that observed in the presence of glucose (Mason et al., 1998). The Hsp30 chaperone is expressed on glucose exhaustion (via Snf1 activation of the Hsf1 transcription factor (Hahn and Thiele, 2004) and inhibits Pma1 activity (Panaretou and Piper, 1992; Piper et al., 1997). Deletion of *HSP30* thus maintains Pma1 activity even in the absence of glucose. Either *PMA1-Δ901* truncation or deletion of *HSP30* results in a 20–30% decrease in *ADH2* expression (Figure 4A). In combination, a dramatic decrease in Snf1 function is observed, as both pathways of Pma1 downregulation are now disabled. These decreases in *ADH2* expression are suppressed by Snf1^{ΔH}, indicating that Pma1 upregulation is signaling via the polyHIS tract (Figure 4A). Similar results were obtained for *ACS1* (Figure S4B) and *JEN1* (Figure S4C) expression. Upregulating Pma1 activity did not diminish phosphorylation of Snf1 at T210 (Figure 4B). However, on shift to ethanol medium Rod1 is degraded in *hsp30Δ PMA1-Δ901* cells (rather than being phosphorylated) – this phenotype is suppressed and normal maximal phosphorylation restored by introduction of Snf1^{ΔH} (Figure 4B), suggesting that Snf1^{ΔH} is not affected by high Pma1 activity.

Upregulating Pma1 activity by deletion of *HSP30* and/or by *PMA1-Δ901* increases the interaction between the NTD (1-391) and CTD (392-633) domains of Snf1. (Figure 4C). However, Pma1 upregulation does not change the low interaction between the NTD and CTD when the polyHIS tract in the NTD is deleted (ΔH), nor the high interaction observed by substitution to tryptophan (W) (Figure 4C), demonstrating that Pma1, through pH regulation, governs the intra-molecular interactions of Snf1.

We also inhibited Pma1 using the organo-selenium compound ebselen (Chan et al., 2007; Young et al., 2010). A low dose treatment (10 μM) does not affect Rod1 dephosphorylation on addition of 2% glucose to ethanol grown cells. However, a high dose (100 μM) of ebselen prevents dephosphorylation of Rod1 in the presence of glucose (Figure 4D). This is suppressed by Snf1^{ΔH} (Figure 4D) showing that Snf1^{ΔH} is not regulated by Pma1 activity. Genetically lowering Pma1 activity by deletion of *EXP1* (resulting in cytoplasmic acidification) results in a marked deceleration of Rod1 dephosphorylation on addition of glucose to ethanol grown cells (Figure 4E).

Ebselen was added to yeast-two hybrid cells on transition to glucose and the interaction between the kinase and regulatory domains of Snf1 monitored. Pma1 inhibition prevents association of Snf1^{NTD} and Snf1^{CTD}. However, Pma1 inhibition does not prevent association of Snf1^{CTD} with Snf1^{NTD-W}, in which the polyHIS tract is substituted with neutral deprotonated tryptophan (Figure 4F). Together, these results demonstrate that the polyhistidine tract in the PKR functions as a PSM. Glucose thus inhibits Snf1 via upregulation of Pma1 activity, causing deprotonation of the polyHIS tract, resulting in its association with the β-subunit binding site.

The polyHIS tract elicits a progressive response

Although the kinase domain of AMPK/Snf1 is highly conserved from yeasts to man, the PKR shows immense variation both in length (53 amino acids in *S. cerevisiae*, 25 amino acids in *Homo sapiens*, 74 amino acids in *Candida parapsilosis*) and composition, with metazoans typically having short unenriched sequences, whereas yeasts and fungi often possess a PKR with enrichment or tracts of histidine (H), asparagine (N) and glutamine (Q) (Figure S1). To investigate the effects of sequence heterogeneity on Snf1 activity, we replaced the first 52 acids of *S. cerevisiae* Snf1 with the equivalent PKR from *Kluyveromyces*, *Saccharomyces* and *Candida* yeasts, all of which contain either histidine enrichment or polyHIS tracts of various lengths. We also created a *S. cerevisiae* PKR with only 4 or 8 polyhistidines. Removal of the PKR or replacement with the *H. sapiens* PKR eliminates Snf1 activity (Figure 5A). Most heterologous PKR chimeras did not drastically affect Snf1 activity, but the PKR from *Kluyveromyces lactis* Fog2 increased Snf1 activity to levels near that of Snf1^{ΔH}. The *K. lactis* PKR contains only two consecutive histidines (with three more scattered); this could explain why it is ineffective in regulating *S. cerevisiae* Snf1. The *S. cerevisiae* 4-histidine construct has a Snf1 activity between that of the wild-type Snf1 (14 histidines) and Snf1^{ΔH}, and the 8-histidine construct has a Snf1 activity between WT (14 histidines) and the 4-histidine mutant. We therefore plotted Snf1 activity as a function of the number of histidines in the PKR and found a strong correlation (Figure 5B). This demonstrates that Snf1 activity progressively decreases on gain of even two consecutive histidines (such as in the PKR of *K. lactis* Fog2).

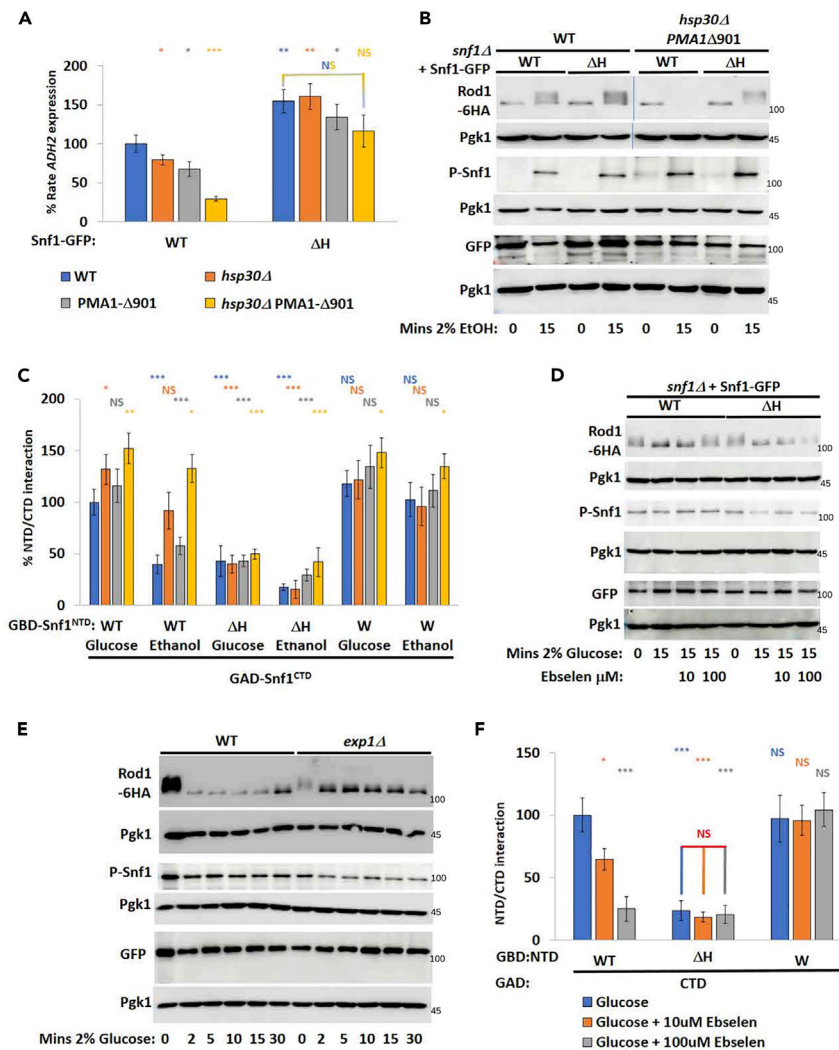


Figure 4. The polyHIS tract of Snf1 is a pH sensing module

(A) *ADH2* expression of *snf1Δ* cells and *snf1 hsp30Δ* cells with *prSNF1::Snf1*-GFP or *prSNF1::Snf1^{ΔH}*-GFP, and with *PMA1* or *PMA1-Δ901*. N = 3. T-tests were conducted against WT (far left, blue). NS = not significant, * = $p \leq 0.05$, ** = $p \leq 0.01$, *** = $p \leq 0.001$.

(B) Rod1-6HA and Snf1 T210 phosphorylation following transfer of cells from 4% glucose to 2% ethanol media for 15 min. Cells were grown and processed as described in materials and methods. Molecular weight markers are indicated to the right of the image in kDa.

(C) Yeast two-hybrid experiment showing interaction of GBD-Snf1^{NTD} and GAD-Snf1^{CTD} in glucose and ethanol media. N = 3. T-test is against WT cells in glucose (far left, blue). NS = not significant, * = $p \leq 0.05$, ** = $p \leq 0.01$, *** = $p \leq 0.001$.

(D) Rod1-6HA phosphorylation following addition of glucose to 2% to ethanol grown cells with indicated concentrations of ebselen. Cells were grown and processed as described in materials and methods.

(E) Rod1-6HA dephosphorylation following addition of glucose to 2% to ethanol grown cells. Cells were grown and processed as described in materials and methods. Molecular weight markers are indicated to the right of the image in kDa.

(F) Yeast two-hybrid experiment to determine interaction between GBD-Snf1^{NTD} and GAD-Snf1^{CTD} in the presence of the indicated concentration of ebselen. N = 3. T-tests were performed against WT glucose without ebselen (far left, blue). NS = not significant, * = $p \leq 0.05$, ** = $p \leq 0.01$, *** = $p \leq 0.001$.

DISCUSSION

The importance of pH as a second messenger for carbon metabolism

Protons are an abundant diffusible signaling molecule that act as a second messenger for highly fermentable carbon sources, both via the plasma membrane ATPase (*Pma1*) and the vacuolar ATPase (*Vma1*), controlling many processes, including membrane biogenesis (Young et al., 2010) and metabolic enzyme

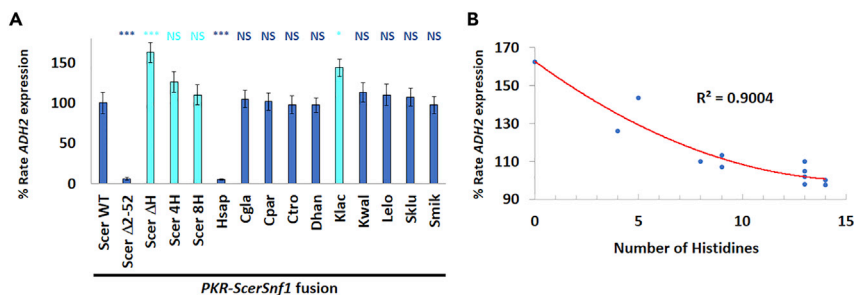


Figure 5. The polyHIS tract elicits a progressive response

(A) *ADH2* expression of *snf1Δ* cells transformed with *Snf1*-GFP plasmids bearing the indicated PKR (see the legend of Figure S1 and Table 2 for details). N = 3. Results which are of note are in turquoise. T-tests were performed against WT glucose (far left, blue). NS = not significant, * = $p \leq 0.05$, ** = $p \leq 0.01$, *** = $p \leq 0.001$.

(B) Number of consecutive histidines in the PKR was plotted against *ADH2* expression using data from (A). R^2 value was calculated by Excel.

aggregation (Petrovska et al., 2014). It is unclear how glucose activates these proton pumps. Pma1 activity decreases extracellular pH, thus activating Gpa2 (which functions as a pH sensor as well as a glucose sensor). Only the fermentable, non-*Snf1* activating sugars glucose, fructose and mannose cause this effect, and other hexoses or disaccharides do not affect pH or PKA activity (Isom et al., 2018). Increased glycolytic flux beyond glucose-6-phosphate increases Vma1 activity leading to activation of PKA (Dechant et al., 2010). Recently, valproate has been shown to decrease glycolytic flux resulting in both increased phosphorylation at T210, and decreased Pma1 activity (Salsaa et al., 2021). Here we have shown that decreasing Pma1 activity is a requirement for *Snf1* activation. Because PKA and *Snf1* reciprocally regulate each other through multiple mechanisms (PKA regulates *Snf1* via inhibitory SUMOylation (Simpson-Lavy et al., 2015), inhibiting Sak1 activity (Barrett et al., 2012), and by controlling Sip1 localization (Hedbacker et al., 2004), whereas *Snf1* inhibits adenyl cyclase (Cyr1) (Nicastro et al., 2015) we can now state that PKA and *Snf1* are also oppositely regulated by pH, ensuring co-ordination of metabolic signaling across the cell.

There are two mechanisms by which Pma1 mediated proton export (and thus cytoplasmic alkalization) is attenuated by glucose deprivation – dephosphorylation of the C-terminal tail (Mason et al., 1998) and Pma1 protein destabilization by Hsp30 (Panaretou and Piper, 1992; Piper et al., 1997). We found that both Pma1 inactivation pathways need to be inhibited (Pma1-Δ901 and *hsp30Δ*) to obtain the maximal inhibition of *Snf1* in ethanol media (Figure 4A). This may suggest that the reduction of Pma1 activity on glucose deprivation may be achieved by either mechanism.

A regulation module that senses pH

The PKR (aa 2-53) is essential for *Snf1* activity (Figures 1 and 2A) despite being heterogenous between species, whereas the kinase domain (aa 54-391) is considerably conserved. We found that substitution with the human PKR (aa 2-26 of AMPK α) renders this fusion inactive. This is probably because of the distal part of the PKR and AMPK β (*Snf4* in *S. cerevisiae*) forming the (allosteric drug and metabolite) ADaM pocket (Calabrese et al., 2014; Jørgensen et al., 2021). This pocket centered around G53 may also explain why the hyperactive ScSnf1^{G53R} mutant suppresses *snf4* (Estruch et al., 1992). It is probable that the human PKR is incompatible with *S. cerevisiae* *Snf4*. Indeed, HsAMPK α does not complement *snf1Δ* in *S. cerevisiae* – although replacement of all of the *Snf1* complex in *S. cerevisiae* with human AMPK α,β,γ can permit growth on non-fermentable carbon sources (Ye et al., 2014).

In this study we have identified a neglected motif in *Snf1*, the polyHIS tract of the PKR, as a Pma1 activity/pH sensing module (PSM) that regulates *Snf1* activity, thus directly linking glucose activation of Pma1 (and thus intracellular alkalization) and inhibition of *Snf1*. Increasing Pma1 activity by deletion of *hsp30* in combination with the PMA1-Δ901 allele lowers *Snf1* activity (Figures 4A, 4B, S4B, and S4C) and decreasing Pma1 activity in glucose results in a deceleration of *Snf1* inactivation (Figures 4D and 4E), with deletion of the PSM suppressing these phenotypes. The polyHIS tract acts by interacting with, and blocking, the β -subunit binding site in the far C-terminal of *Snf1* (Figures 3B, 3C, and 3D); preventing *Snf1* activation and entry into

the nucleus (Figures 2A and 2C). By substituting other poly amino-acids for the polyHIS we found that Snf1^A mimics deletion of the polyHIS tract, whereas aromatic, neutral amino acids (Snf1^F and Snf1^W) cause the kinase and regulatory domains of Snf1 to maintain their interaction even in the absence of glucose, mimicking deprotonated polyHIS as would be found in glucose-grown cells. Because the aromatic amino acids mimic deprotonated histidine, but mutation to alanine is congruent with a histidine-null phenotype, it is likely that π -bond stacking of the polyHIS is interacting with the β -subunit binding site in the C-terminal of Snf1. Deletion of the polyHIS tract results in Snf1 being inactivated faster in glucose (Figure 2F), probably because of a loss of this level of regulation.

The PSM binds (in glucose) and is released from (in ethanol) the β -subunit binding site because of its deprotonation (in glucose) and protonation (in ethanol). This was determined by upregulating Pma1 activity in ethanol (*PMA1- Δ 901* and *hsp30 Δ*) (Figure 4C) or by inhibiting Pma1 with ebselen in glucose (Figure 4F), with phenotypes being suppressed by Snf1^{AH} or Snf1^W appropriately. This establishes a direct, distinct signaling pathway from glucose to Pma1 activity resulting in deprotonation of Snf1 and thus Snf1 inhibition.

Substitution of the PSM with arginine resulted in an N-terminal truncation of Snf1 (Figure 2E) and much reduced activity (Figures 2A, S2A, and S2B). In most ways Snf1^R behaves like Snf1^F, but isolated PKR^R interacts well with the KD in ethanol media – probably because of the high positive charge interacting with phosphorylated T210.

Although how exactly glucose regulates T210 activation loop phosphorylation remains unclear, it is important to note that even without a PSM, phosphorylation at T210 is still required for Snf1 activity (Figure 2A). Moreover, the interaction of the PKR with the kinase domain in the absence of glucose also requires phosphorylation at T210 (Figure 3E). Furthermore, mutation of the polyHIS tract does not prevent phosphorylation at T210 on glucose withdrawal, giving rise to a situation whereby Snf1 can be phosphorylated at T210 (Figure 2E), but a mutation in the polyHIS tract prevents dissociation of the kinase and regulatory domains (Figure 3C) and thus Snf1 kinase activity is still inhibited (Figure 2A). Similarly, although modulation of Pma1 activity affects Snf1 target gene expression (Figures 4A, S4B, and S4C) and Rod1 phosphorylation (Figures 4B, 4D, and 4E); regulation of Snf1 phosphorylation at T210 is unaffected. In other words, our work shows that Snf1 activation requires two events: T210 phosphorylation and protonation of the polyHIS tract. Of importance, a corollary from these results is that experiments showing T210 phosphorylation do not automatically demonstrate the presence of an active Snf1.

The data allows a reconstruction of a mechanism of Snf1 regulation by Pma1 activity (Figure 6). In the **absence** of glucose:

1. Pma1 activity is inhibited, resulting in acidification of the cytoplasm and polyHIS protonation.
2. Snf1 is phosphorylated at T210 and de-SUMOylated (independently from polyHIS protonation).
3. The protonated polyHIS tract dissociates from the β -subunit binding site (because of the higher positive charge) and interacts with T210 phosphorylated kinase domain.
4. β -subunits can now interact with Snf1. Snf1 is active and enters the nucleus.
5. Snf1 activity increases Hsp30 levels, further inhibiting Pma1.

The three mechanisms of Snf1 activation on glucose deprivation thus identified: protonation of the polyHIS tract in the PSM, phosphorylation at T210 and de-SUMOylation of K549, are all required for Snf1 activity, and are all independent from each other. Thus Snf1 acts as a signal coordinator, similar to the integration of glucose, nitrogen and phosphate sensing by Rim15 (Swinnen et al., 2006).

PolyHIS sensing is progressive

An emergent theme is that histidines can act as pH sensors, such as RasGRP1 in *H. sapiens* at a single histidine H212 (Vercoulen et al., 2017) or utilizing multiple histidine residues in PsaF of *Y. pestis* (Quinn et al., 2021) or the human prion PrP (Zahn, 2003).

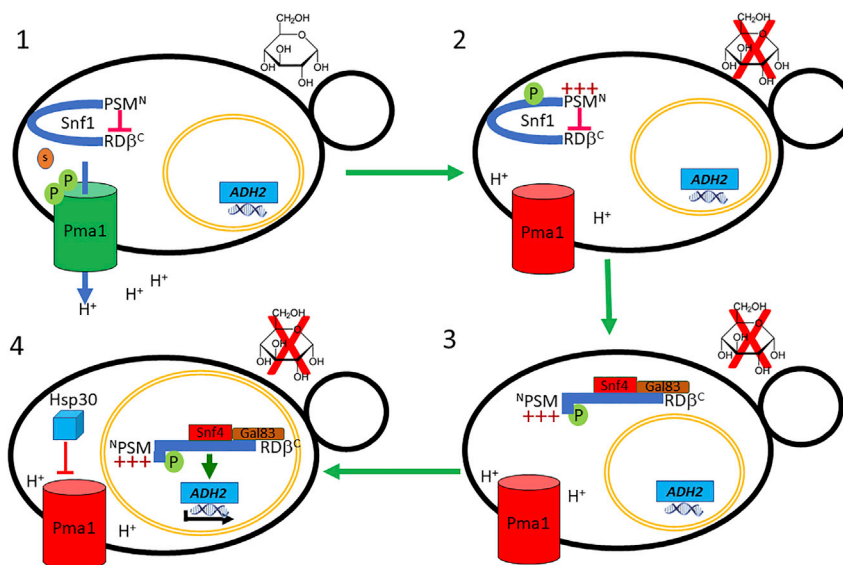


Figure 6. Model of the mechanism by which pH regulates Snf1.

1. In glucose medium PMA1 is phosphorylated and pumps protons out of the cell resulting in polyHIS deprotonation (mimicked by Snf1^F and Snf1^W).
2. On glucose deprivation, PMA1 is dephosphorylated and much less active. The polyHIS of Snf1 becomes protonated and Snf1 is phosphorylated at T210. These events are independent.
3. The protonated polyHIS tract disengages from the β -subunit binding site, and Snf4 and a β -subunit (Gal83, Sip1, Sip2) can interact.
4. Snf1-Snf4-Gal83 enters the nucleus resulting in expression of respiration genes such as *ADH2* and *HSP30*. Hsp30 further inhibits Pma1. The nucleus in this panel is enlarged for clarity only.

It is possible that pH sensing of Snf1 arises from the aggregate charge changes of the histidines in the PSM. We determined that the number of histidines in the PKR inversely correlates with Snf1 activity (Figures S1, 5A, and 5B). Thus, it appears that the crucial determinant of pH sensing by polyHIS in Snf1 is the number of local histidines, which may implicate π -bond stacking as the molecular interaction with the β -subunit binding site in the regulatory domain.

PSMs in the proteome

The polyHIS motif of the PSM is very rare. In *S. cerevisiae* only 12 other proteins contain polyHIS stretches with more than 7 histidines (H^{7+} representing 0.25% of the *S. cerevisiae* proteome [assuming 5815 proteins (Engel et al., 2014)] In contrast, 91 (1.6%) of *S. cerevisiae* proteins contain poly Q^{7+} . The human genome contains 95 poly H^{7+} proteins representing 0.47% of the proteome (assuming 20,352 protein-encoding genes (Perteau et al., 2018)) whereas poly Q^{7+} proteins number 709 (3.5% of the proteome). The ratio of proteins with poly H^{7+} to proteins with poly Q^{7+} is thus constant between yeast and humans. The proteins containing poly H^{7+} in yeast are diverse and do not seem to have a common function, although 4 of the 12 are involved in metabolism and stress response (*SNF1*, *TAX4*, *ROM2*, *BAG7*). However, in humans, an enrichment for voltage-gated channels is observed – this could permit a progressive change in voltage to accumulate in the histidines and when a threshold is reached to effect a conformational/interactional change. Indeed, multiple histidine residues have been found to be important in the human voltage-gated channel Hv1 (Zhao et al., 2015; Cherny et al., 2018) but analysis of histidines as a group has yet to be performed.

Although Snf1 has been an intensively investigated protein in the last 40 years, the function of the rarely occurring polyHIS tract at the N-terminus has hitherto not been elucidated. We have found that this region constitutes a PSM, which enables a direct progressive regulation of Snf1 by pH changes arising from the presence of glucose. Roles for pH sensing modules, such as the one we have found for the yeast AMPK ortholog are likely to govern cellular processes in many organisms, as pH variations are ubiquitous, and affected by nutrient availability and cellular metabolism.

Table 1. Yeast strains

Number	Name	Genotype	From
1	WT	W303 MATa <i>ade2-1 his3-11,15 trp1-1 leu2-3,112 ura3-1 rad5-535 bud4</i>	Lab collection
2	<i>snf1</i>	As 1 <i>snf1::HYG</i>	E. Young (Ratnakumar et al., 2009)
3	<i>snf1 ADE2</i>	As 1 <i>snf1::HYG ADE2</i>	This study
4	<i>reg1</i>	As 1 MATα <i>reg1::NAT</i>	E. Young (Ratnakumar et al., 2009)
5	<i>snf1 reg1</i>	As 1 <i>snf1::HYG reg1::NAT</i>	E. Young (Ratnakumar et al., 2009)
6	<i>snf1 mig1</i>	As 1 <i>snf1::HYG mig1::KAN</i>	This study
7	<i>snf1 hsp30</i>	As 1 <i>snf1::HYG hsp30::NAT</i>	This study
8	<i>snf1 Rod1-6HA</i>	As 1 <i>snf1::HYG Rod1-6HA::NAT</i>	This study
9	<i>snf1 Rod1-6HA hsp30</i>	As 1 <i>snf1::HYG Rod1-6HA::NAT hsp30::KAN</i>	This study
10	<i>snf1 Rod1-6HA exp1</i>	As 1 <i>snf1::HYG Rod1-6HA::NAT exp1::KAN</i>	This study
11	PJ694	<i>trp1-901 leu2-3,112, ura3-52, his3Δ200, gal4Δ, gal80Δ, prGAL2:ADE2 lys2::prGAL1::HIS3 met2::prGAL7-LacZ</i>	Lab collection
12	Y2H <i>hsp30</i>	As 8 <i>hsp30::NAT</i>	

All *S. cerevisiae* strains are in the W303 background except PJ694 (for Yeast 2-Hybrid assays).

Yeast strains, plasmids and oligonucleotides used

The strains used in this study are listed in Table 1. Plasmids are shown in Table 2. Oligonucleotides are listed in Table 3.

Limitations of the study

We have shown that Snf1 is inhibited by genetically upregulating Pma1 activity which causes intracellular alkalization, and also that Snf1 remains more active when Pma1 activity is lowered (causing intracellular acidification), both chemically and genetically. Future experiments should directly measure the internal pH. We acknowledge that our model of internal and external interactions of Snf1 is inferred from yeast two-hybrid data and not by other more direct techniques. Future experiments could include co-immunoprecipitations and biophysical measurements of protein dynamics.

STAR★METHODS

Detailed methods are provided in the online version of this paper and include the following:

- KEY RESOURCES TABLE
- RESOURCE AVAILABILITY
 - Lead contact
 - Materials availability
 - Data and code availability
- EXPERIMENTAL MODEL AND SUBJECT DETAILS
 - Yeasts, plasmids, and growth conditions
- METHOD DETAILS
 - β-galactosidase assays for gene expression
 - Yeast 2-hybrid experiments
 - Western blots
 - Microscopy
 - Serial dilutions
- QUANTIFICATION AND STATISTICAL ANALYSIS

SUPPLEMENTAL INFORMATION

Supplemental information can be found online at <https://doi.org/10.1016/j.isci.2022.105083>.

Table 2. Plasmids

Number	Genotype	Backbone	Source/Notes
152	Snf1-GFP	Prs313	M. Carlson (Vincent et al., 2001)
728	Snf1-GFP	Prs315	Marker switch of 152
847	Snf1-ΔH-GFP	Prs315	polyHIS of 728 deleted
1244	Snf1-4H-GFP	Prs315	4 polyhistidines in PKR (by PCR from 847)
1248	Snf1-8H-GFP	Pr315	8 polyhistidines in PKR (by PCR from 847)
742	Snf1-A-GFP	Prs315	Alanine substituted for histidine in PKR of 728
852	Snf1-F-GFP	Prs315	Phenylalanine substituted for histidine in PKR of 728
744	Snf1-K-GFP	Prs315	Lysine substituted for histidine in PKR of 728
1257	Snf1-R-GFP	Prs315	Arginine substituted for histidine in PKR of 728
745	Snf1-W-GFP	Prs315	Trptophan substituted for histidine in PKR of 728
731	Snf1-Y-GFP	Prs315	Tyrosine substituted for histidine in PKR of 728
982	Snf1-Δ2-52-GFP	Prs315	Pre-kinase region deleted
846	Snf1-T210A-GFP	Prs315	T210A mutation in 728
1 or 919	<i>prADH2::LacZ</i>	Prs316	E. Young (Ratnakumar et al., 2009)
63	<i>prADH2::LacZ</i>	Prs313	Marker switch of 1
164	<i>prADH2::LacZ</i>	Prs315	Marker switch of 1
240	<i>prACS1::LacZ</i>	2μ URA3	H.J. Schüller (Kratzer and Schüller, 1995)
706	<i>prJEN1::LacZ</i>	Yep358	B. Guiard (Lodi et al., 2002)
526	Nup49-Cherry	Prs314	M. Lisby (Germann et al., 2014)
589	Nup49-Cherry	Prs316	Marker switch of 526
590	Nup49-Cherry	Prs315	Marker switch of 526
816	Snf1-3HA	Prs313	M. Carlson (Liu et al., 2011)
817	Snf1- K84R-3HA	Prs313	M. Carlson (Liu et al., 2011)
818	Snf1- T210A 3HA	Prs313	M. Carlson (Liu et al., 2011)
819	Snf1-ΔH-3HA	Prs313	polyHIS of 816 deleted
820	Snf1-A-3HA	Prs313	Alanine substituted for histidine in 816
835	Snf1-ΔH-T210A-3HA	Prs313	polyHIS of 818 deleted
1234	Pma1	Prs314	Pma1 inserted into prs314
1238	Pma1-Δ901	Prs314	Final 18aa of Pma1 deleted

Yeast 2-hybrid plasmids

153	<i>prADH1::GAD</i>	LEU2, 2μ	pACT2 Yeast 2-hybrid empty vector
154	<i>prADH1::GBD</i>	TRP1, 2μ	pGBT9 Yeast 2-hybrid empty vector
155	<i>prADH1::GBD</i>	URA3, 2μ	pGBU9 Yeast 2-hybrid empty vector
753	GAD-Snf4	LEU2, 2μ	Snf4 in 153
755	GAD-Sip1	LEU2, 2μ	Sip1 in 153
756	GAD-Sip2	LEU2, 2μ	Sip2 in 153
757	GAD-Gal83	LEU2, 2μ	Gal83 in 153
762	GBD-Snf1	URA3, 2μ	Snf1 in 155
763	GBD-Snf1 K84R	URA3, 2μ	Snf1 K84R in 155
764	GBD-Snf1 T210A	URA3, 2μ	Snf1 T210A in 155
789	GBD-Snf1 ΔH	URA3, 2μ	polyHIS deletion of 762
779	GBD-Snf1 A	URA3, 2μ	Alanine substituted for polyHIS in 762
801	GBD-Snf1 F	URA3, 2μ	Phenylalanine substituted for polyHIS in 762
787	GBD-Snf1 R	URA3, 2μ	Arginine substituted for polyHIS in 762
765	GBD-Snf1 W	URA3, 2μ	Tryptophan substituted for polyHIS in 762

(Continued on next page)

Table 2. Continued

Number	Genotype	Backbone	Source/Notes
768	GBD-Snf1 Y	URA3, 2 μ	Tyrosine substituted for polyHIS in 762
781	GBD-Snf1 1-391	URA3, 2 μ	Snf1 1-391 in 155
786	GBD-Snf1 392-633	URA3, 2 μ	Snf1 392-633 in 155
810	GBD-Snf1 392-633 K549R	URA3, 2 μ	Snf1 392-633 in 155
791	GAD-Snf1 392-633	LEU2, 2 μ	Snf1 392-633 in 153
822	GAD-Snf1 392-633 K549R	LEU2, 2 μ	Snf1 392-633 K549R in 153
795	GBD-Snf1 1-391 Δ H	URA3, 2 μ	Snf1 1-391 Δ H in 155
807	GBD-Snf1 1-391 A	URA3, 2 μ	Snf1 1-391 A in 155
805	GBD-Snf1 1-391 F	URA3, 2 μ	Snf1 1-391 F in 155
798	GBD-Snf1 1-391 R	URA3, 2 μ	Snf1 1-391 R in 155
785	GBD-Snf1 1-391 W	URA3, 2 μ	Snf1 1-391 W in 155
783	GBD-Snf1 1-391 Y	URA3, 2 μ	Snf1 1-391 Y in 155
828	GBD-Snf1 1-53	URA3, 2 μ	Snf1 1-53 in 155
836	GBD-Snf1 1-53 Δ H	URA3, 2 μ	Snf1 1-53 Δ H in 155
829	GBD-Snf1 1-53 A	URA3, 2 μ	Snf1 1-53 A in 155
830	GBD-Snf1 1-53 F	URA3, 2 μ	Snf1 1-53 F in 155
831	GBD-Snf1 1-53 R	URA3, 2 μ	Snf1 1-53 R in 155
837	GBD-Snf1 1-53 W	URA3, 2 μ	Snf1 1-53 W in 155
836	GBD-Snf1 1-53 Y	URA3, 2 μ	Snf1 1-53 Y in 155
844	GAD-Snf1 54-391	LEU2, 2 μ	Snf1 54-391 in 153
853	GAD-Snf1 54-391 K84R	LEU2, 2 μ	Snf1 54-391 K84R in 153
860	GAD-Snf1 54-391 T210A	LEU2, 2 μ	Snf1 54-391 T210A in 153
954	GAD-Snf1 54-391 T210E	LEU2, 2 μ	Mutagenesis of 844
827	GAD-Snf1 392-513	LEU2, 2 μ	Snf1 392-513 in 153
826	GAD-Snf1 514-633	LEU2, 2 μ	Snf1 514-633 in 153
825	GAD-Snf1 514-633 K549R	LEU2, 2 μ	Snf1 514-633 K549R in 153
Pre-kinase regions from other species. Amino acids 1–52 removed from plasmid 728 <i>prScerSNF1::ScerSNF1-GFP</i> and replaced by:			
893	<i>Ctro</i>	Prs315	1-52 from <i>C. tropicalis</i>
894	<i>Klac</i>	Prs315	1-32 from <i>K. lactis</i> Fog2
895	<i>Kwal</i>	Prs315	1-28 from <i>K. waltii</i>
896	<i>Lelo</i>	Prs315	1-71 from <i>L. elongisporans</i>
898	<i>Cpar</i>	Prs315	1-73 from <i>C. parapsilosis</i>
904	<i>Cgla</i>	Prs315	1-34 from <i>C. glabrata</i>
945	<i>Hsap</i>	Prs315	1-24 from <i>H. sapiens</i>
981	<i>Dhan</i>	Prs315	1-52 from <i>D. hansenii</i>
985	<i>Smik</i>	Prs315	1-40 from <i>S. mikatae</i>
986	<i>Sklu</i>	Prs315	1-29 from <i>S. kluyveri</i>

ACKNOWLEDGMENTS

We thank all members of the Kupiec lab for support and ideas. We thank Marian Carlson, Elton Young, Michael Lisby for strains and plasmids. This work was supported by grants to M.K. from the Israel Science Foundation, the Israel Cancer Research Fund and the Minerva Stiftung.

AUTHOR CONTRIBUTIONS

K.S.-L. and M.K. conceived the work; K.S.-L. conducted the experiments; K.S.-L. and M.K. wrote the article.

Table 3. Continued

Name	Description	Sequence
M68*	4H/8H-5	GGCGGAAGCAACTCGACG
M69*	4H-3	ATGGTGATGGTGGCTAGAATTTGCATTGGCAGGTGCTGTG
M70*	8H-3	ATGGTGATGGTGGTGGTGGTGGCTAGAATTTGCATTGGCAGGTGCTGTG
Pma1 truncation		
C292	PMA1-5	Gaattgtaatacgaactactatagggcgaattggagctccgcttctgaaacggagaaac
C293	PMA1-3	Ctctactcattaggcaccacaggctttacattatgctccgctccgtaaaggatttcgcggagg
C294*	Pma1-trunc5	TAAcctgtgaagtagcatttaac
C295*	Pma1-trunc3	GACACTTCTGGTAGACTTCTTTTC

All oligonucleotides were ordered from Sigma. Desalted, no purification. Upon receipt they were resuspended to 100 μ M in 5 mM Tris (pH 8.5). Primers marked with an asterisk were phosphorylated using phosphonucleotide kinase before use.

DECLARATION OF INTERESTS

The authors declare no competing interests.

INCLUSION AND DIVERSITY

We support inclusive, diverse, and equitable conduct of research.

Received: January 31, 2022

Revised: August 12, 2022

Accepted: September 1, 2022

Published: October 21, 2022

REFERENCES

- Ahn, B.-E., and Baker, T.A. (2016). Oxidation without substrate unfolding triggers proteolysis of the peroxide-sensor. *Proc. Natl. Acad. Sci. USA* 113, E23–E31.
- Amodeo, G.A., Rudolph, M.J., and Tong, L. (2007). Crystal structure of the heterotrimer core of *Saccharomyces cerevisiae* AMPK homologue SNF1. *Nature* 449, 492–495.
- Ariño, J., Ramos, J., and Sychrova, H. (2019). Monovalent cation transporters at the plasma membrane in yeasts. *Yeast* 36, 177–193.
- Barrett, L., Orlova, M., Maziarz, M., and Kuchin, S. (2012). Protein kinase A contributes to the negative control of Snf1 protein kinase in *Saccharomyces cerevisiae*. *Eukaryot. Cell* 11, 119–128.
- Becuwe, M., Vieira, N., Lara, D., Gomes-Rezende, J., Soares-Cunha, C., Casal, M., Haguenaer-Tsapis, R., Vincent, O., Paiva, S., and Léon, S. (2012). A molecular switch on an arrestin-like protein relays glucose signaling to transporter endocytosis. *J. Cell Biol.* 196, 247–259.
- Burggren, W., and Bautista, N. (2019). Invited review: development of acid-base regulation in vertebrates. *Comparative biochemistry and physiology. Comp. Biochem. Physiol. Mol. Integr. Physiol.* 236, 110518.
- Calabrese, M.F., Rajamohan, F., Harris, M.S., Caspers, N.L., Magyar, R., Withka, J.M., Wang, H., Borzilleri, K.A., Sahasrabudhe, P.V., Hoth, L.R., et al. (2014). Structural Basis for AMPK Activation: Natural and Synthetic Ligands Regulate Kinase Activity from Opposite Poles by Different Molecular Mechanisms. *Structure* 22, 1161–1172.
- Celenza, J.L., and Carlson, M. (1989). Mutational analysis of the *Saccharomyces cerevisiae* SNF1 protein kinase and evidence for functional interaction with the SNF4 protein. *Mol. Cell Biol.* 9, 5034–5044.
- Chan, G., Hardej, D., Santoro, M., Lau-Cam, C., and Billack, B. (2007). Evaluation of the antimicrobial activity of ebselen: role of the yeast plasma membrane H⁺-ATPase. *J. Biochem. Mol. Toxicol.* 21, 252–264.
- Charbon, G., Breunig, K.D., Wattiez, R., Vandenhaute, J., and Noël-Georis, I. (2004). Key role of Ser562/661 in Snf1-dependent regulation of Cat8p in *Saccharomyces cerevisiae* and *Kluyveromyces lactis*. *Mol. Cell Biol.* 24, 4083–4091.
- Cherny, V.V., Morgan, D., Thomas, S., Smith, S.M.E., and DeCoursey, T.E. (2018). Histidine168 is crucial for Δ pH-dependent gating of the human voltage-gated proton channel, hHV1. *J. Gen. Physiol.* 150, 851–862.
- Cosse, M., and Seidel, T. (2021). Plant proton pumps and cytosolic pH-homeostasis. *Front. Plant Sci.* 12, 672873.
- Dechant, R., Binda, M., Lee, S.S., Pelet, S., Winderickx, J., and Peter, M. (2010). Cytosolic pH is a second messenger for glucose and regulates the PKA pathway through V-ATPase. *EMBO J.* 29, 2515–2526.
- Elbing, K., Rubenstein, E.M., McCartney, R.R., and Schmidt, M.C. (2006). Subunits of the Snf1 kinase heterotrimer show interdependence for association and activity. *J. Biol. Chem.* 281, 26170–26180.
- Engel, S.R., Dietrich, F.S., Fisk, D.G., Binkley, G., Balakrishnan, R., Costanzo, M.C., Dwight, S.S., Hitz, B.C., Karra, K., Nash, R.S., et al. (2014). The Reference Genome Sequence of *Saccharomyces cerevisiae*: then and Now. *G3 (Bethesda, Md.)* 4, 389–398.
- Eraso, P., Mazón, M.J., and Portillo, F. (2006). Yeast protein kinase Ptk2 localizes at the plasma membrane and phosphorylates in vitro the C-terminal peptide of the H⁺-ATPase. *Biochim. Biophys. Acta* 1758, 164–170.
- Estruch, F., Treitel, M.A., Yang, X., and Carlson, M. (1992). N-terminal mutations modulate yeast SNF1 protein kinase function. *Genetics* 132, 639–650.
- Ferreira, C., van Voorst, F., Martins, A., Neves, L., Oliveira, R., Kielland-Brandt, M.C., Lucas, C., and Brandt, A. (2005). A member of the sugar transporter family, Stl1p is the glycerol/H⁺ symporter in *Saccharomyces cerevisiae*. *Mol. Biol. Cell* 16, 2068–2076.

- Fujita, S., Sato, D., Kasai, H., Ohashi, M., Tsukue, S., Takekoshi, Y., Gomi, K., and Shintani, T. (2018). The C-terminal region of the yeast monocarboxylate transporter Jen1 acts as a glucose signal-responding degranon recognized by the α -arrestin Rod1. *J. Biol. Chem.* **293**, 10926–10936.
- García-Arranz, M., Maldonado, A.M., Mazón, M.J., and Portillo, F. (1994). Transcriptional control of yeast plasma membrane H⁺-ATPase by glucose. Cloning and characterization of a new gene involved in this regulation. *J. Biol. Chem.* **269**, 18076–18082.
- Germann, S.M., Schramke, V., Pedersen, R.T., Gallina, I., Eckert-Boulet, N., Oestergaard, V.H., and Lisby, M. (2014). TopBP1/Dpb11 binds DNA anaphase bridges to prevent genome instability. *J. Cell Biol.* **204**, 45–59.
- Geva, Y., Crissman, J., Arakel, E.C., Gómez-Navarro, N., Chuartzman, S.G., Stahmer, K.R., Schwappach, B., Miller, E.A., and Schuldiner, M. (2017). Two novel effectors of trafficking and maturation of the yeast plasma membrane H⁺-ATPase. *Traffic (Copenhagen, Denmark)* **18**, 672–682.
- Ghillebert, R., Swinnen, E., Wen, J., Vandesteene, L., Ramon, M., Norga, K., Rolland, F., and Winderickx, J. (2011). The AMPK/Snf1/SnrK1 fuel gauge and energy regulator: structure, function and regulation. *FEBS J.* **278**, 3978–3990.
- Goossens, A., de La Fuente, N., Forment, J., Serrano, R., and Portillo, F. (2000). Regulation of yeast H⁺-ATPase by protein kinases belonging to a family dedicated to activation of plasma membrane transporters. *Mol. Cell Biol.* **20**, 7654–7661.
- Hahn, J.-S., and Thiele, D.J. (2004). Activation of the *Saccharomyces cerevisiae* heat shock transcription factor under glucose starvation conditions by Snf1 protein kinase. *J. Biol. Chem.* **279**, 5169–5176.
- Hedbacker, K., Townley, R., and Carlson, M. (2004). Cyclic AMP-dependent protein kinase regulates the subcellular localization of Snf1-Sip1 protein kinase. *Mol. Cell Biol.* **24**, 1836–1843.
- Hong, S.-P., Leiper, F.C., Woods, A., Carling, D., and Carlson, M. (2003). Activation of yeast Snf1 and mammalian AMP-activated protein kinase by upstream kinases. *Proc. Natl. Acad. Sci. USA* **100**, 8839–8843.
- Isom, D.G., Page, S.C., Collins, L.B., Kapolka, N.J., Taghon, G.J., and Dohlman, H.G. (2018). Coordinated regulation of intracellular pH by two glucose-sensing pathways in yeast. *J. Biol. Chem.* **293**, 2318–2329.
- Jiang, R., and Carlson, M. (1996). Glucose regulates protein interactions within the yeast SNF1 protein kinase complex. *Genes Dev.* **10**, 3105–3115.
- Jiang, R., and Carlson, M. (1997). The Snf1 protein kinase and its activating subunit, Snf4, interact with distinct domains of the Sip1/Sip2/Gal83 component in the kinase complex. *Mol. Cell Biol.* **17**, 2099–2106.
- Jørgensen, N.O., Kjøbsted, R., Larsen, M.R., Birk, J.B., Andersen, N.R., Albuquerque, B., Schjerling, P., Miller, R., Carling, D., Pehmøller, C.K., and Wojtaszewski, J.F.P. (2021). Direct small molecule ADaM-site AMPK activators reveal an AMPK γ 3-independent mechanism for blood glucose lowering. *Mol. Metab.* **51**, 101259.
- Kane, P.M. (2016). Proton transport and pH control in fungi. *Adv. Exp. Med. Biol.* **892**, 33–68.
- Knop, M., Siegers, K., Pereira, G., Zachariae, W., Winsor, B., Nasmyth, K., and Schiebel, E. (1999). Epitope tagging of yeast genes using a PCR-based strategy: more tags and improved practical routines. *Yeast* **15**, 963–972.
- Kratzer, S., and Schüller, H.J. (1995). Carbon source-dependent regulation of the acetyl-coenzyme A synthetase-encoding gene *ACSI* from *saccharomyces cerevisiae*. *Gene* **161**, 75–79.
- Lagadic-Gossmann, D., Huc, L., and Lecœur, V. (2004). Alterations of intracellular pH homeostasis in apoptosis: origins and roles. *Cell Death Differ.* **11**, 953–961.
- Lagunas, R. (1993). Sugar transport in *Saccharomyces cerevisiae*. *FEMS Microbiol. Rev.* **10**, 229–242.
- Liao, S.-M., Du, Q.-S., Meng, J.-Z., Pang, Z.-W., and Huang, R.-B. (2013). The multiple roles of histidine in protein interactions. *Chem. Cent. J.* **7**, 44.
- Liu, Y., Xu, X., and Carlson, M. (2011). Interaction of SNF1 protein kinase with its activating kinase Sak1. *Eukaryot. Cell* **10**, 313–319.
- Llopis-Torregrosa, V., Ferri-Blázquez, A., Adam-Artigues, A., Deffontaines, E., van Heusden, G.P.H., and Yenush, L. (2016). Regulation of the yeast Hxt6 hexose transporter by the Rod1 α -arrestin, the Snf1 protein kinase, and the Bmh2 14-3-3 protein. *J. Biol. Chem.* **291**, 14973–14985.
- Lodi, T., Fontanesi, F., and Guiard, B. (2002). Coordinate regulation of lactate metabolism genes in yeast: the role of the lactate permease gene *JEN1*. *Mol. Genet. Genomics.* **266**, 838–847.
- Loewen, S.K., Ng, A.M.L., Mohabir, N.N., Baldwin, S.A., Cass, C.E., and Young, J.D. (2003). Functional characterization of a H⁺/nucleoside co-transporter (CaCNT) from *Candida albicans*, a fungal member of the concentrative nucleoside transporter (CNT) family of membrane proteins. *Yeast* **20**, 661–675.
- Ma, H., Kunes, S., Schatz, P.J., and Botstein, D. (1987). Plasmid construction by homologous recombination in yeast. *Gene* **58**, 201–216.
- Martínez-Muñoz, G.A., and Kane, P. (2008). Vacuolar and plasma membrane proton pumps collaborate to achieve cytosolic pH homeostasis in yeast. *J. Biol. Chem.* **283**, 20309–20319.
- Mason, A.B., Kardos, T.B., and Monk, B.C. (1998). Regulation and pH-dependent expression of a bilaterally truncated yeast plasma membrane H⁺-ATPase. *Biochim. Biophys. Acta* **1372**, 261–271.
- Mazón, M.J., Eraso, P., and Portillo, F. (2015). Specific phosphoantibodies reveal two phosphorylation sites in yeast Pma1 in response to glucose. *FEMS Yeast Res.* **15**, fov030.
- Munder, M.C., Midtvedt, D., Franzmann, T., Nüske, E., Otto, O., Herbig, M., Ulbricht, E., Müller, P., Taubenberger, A., Maharana, S., et al. (2016). A pH-driven transition of the cytoplasm from a fluid- to a solid-like state promotes entry into dormancy. *Elife* **5**, e09347.
- Nicastro, R., Tripodi, F., Gaggini, M., Castoldi, A., Reghellin, V., Nonnis, S., Tedeschi, G., and Coccetti, P. (2015). Snf1 phosphorylates adenylate cyclase and negatively regulates protein kinase A-dependent transcription in *Saccharomyces cerevisiae*. *J. Biol. Chem.* **290**, 24715–24726.
- Orij, R., Postmus, J., Ter Beek, A., Brul, S., and Smits, G.J. (2009). In vivo measurement of cytosolic and mitochondrial pH using a pH-sensitive GFP derivative in *Saccharomyces cerevisiae* reveals a relation between intracellular pH and growth. *Microbiology (Reading, England)* **155**, 268–278.
- Orlova, M., Barrett, L., and Kuchin, S. (2008). Detection of endogenous Snf1 and its activation state: application to *Saccharomyces* and *Candida* species. *Yeast* **25**, 745–754.
- Panaretou, B., and Piper, P.W. (1992). The plasma membrane of yeast acquires a novel heat-shock protein (hsp30) and displays a decline in proton-pumping ATPase levels in response to both heat shock and the entry to stationary phase. *Eur. J. Biochem.* **206**, 635–640.
- Pertea, M., Shumate, A., Pertea, G., Varabyou, A., Breitwieser, F.P., Chang, Y.-C., Madugundu, A.K., Pandey, A., and Salzberg, S.L. (2018). CHESS: a new human gene catalog curated from thousands of large-scale RNA sequencing experiments reveals extensive transcriptional noise. *Genome Biol.* **19**, 208.
- Petrovska, I., Nüske, E., Munder, M.C., Kulasegaran, G., Malinowska, L., Kroschwald, S., Richter, D., Fahmy, K., Gibson, K., Verbavatz, J.-M., and Alberti, S. (2014). Filament formation by metabolic enzymes is a specific adaptation to an advanced state of cellular starvation. *eLife*. <https://doi.org/10.7554/eLife.02409>.
- Piper, P.W., Ortiz-Calderon, C., Holyoak, C., Coote, P., and Cole, M. (1997). Hsp30, the integral plasma membrane heat shock protein of *Saccharomyces cerevisiae*, is a stress-inducible regulator of plasma membrane H⁺-ATPase. *Cell Stress Chaperones* **2**, 12–24.
- Quinn, J.D., Weening, E.H., and Miller, V.L. (2021). PsaF is a membrane-localized pH sensor that regulates *psaA* expression in *Yersinia pestis*. *J. Bacteriol.* **203**, e0016521.
- Rao, R., Drummond-Barbosa, D., and Slayman, C.W. (1993). Transcriptional regulation by glucose of the yeast PMA1 gene encoding the plasma membrane H⁺-ATPase. *Yeast* **9**, 1075–1084.
- Ratnakumar, S., Kacherovsky, N., Arms, E., and Young, E.T. (2009). Snf1 controls the activity of *adr1* through dephosphorylation of Ser230. *Genetics* **182**, 735–745.
- Ruiz, A., Xu, X., and Carlson, M. (2013). Ptc1 protein phosphatase 2C contributes to glucose regulation of SNF1/AMP-activated protein kinase (AMPK) in *Saccharomyces cerevisiae*. *J. Biol. Chem.* **288**, 31052–31058.

- Saliba, E., Evangelinos, M., Gournas, C., Corrillon, F., Georis, I., and André, B. (2018). The yeast H⁺-ATPase Pma1 promotes Rag/Gtr-dependent TORC1 activation in response to H⁺-coupled nutrient uptake. *Elife* 7, e31981.
- Salsaa, M., Aziz, K., Lazcano, P., Schmidtke, M.W., Tarsio, M., Hüttemann, M., Reynolds, C.A., Kane, P.M., and Greenberg, M.L. (2021). Valproate activates the Snf1 kinase in *Saccharomyces cerevisiae* by decreasing the cytosolic pH. *J. Biol. Chem.* 297, 101110.
- Sanz, P., Alms, G.R., Haystead, T.A., and Carlson, M. (2000). Regulatory interactions between the Reg1-Glc7 protein phosphatase and the Snf1 protein kinase. *Mol. Cell Biol.* 20, 1321–1328.
- Serrano, R., Kielland-Brandt, M.C., and Fink, G.R. (1986). Yeast plasma membrane ATPase is essential for growth and has homology with (Na⁺ + K⁺), K⁺- and Ca²⁺-ATPases. *Nature* 319, 689–693.
- Simpson-Lavy, K.J., Bronstein, A., Kupiec, M., and Johnston, M. (2015). Cross-talk between carbon metabolism and the DNA damage response in *S. cerevisiae*. *Cell Rep.* 12, 1865–1875.
- Simpson-Lavy, K.J., and Johnston, M. (2013). SUMOylation regulates the SNF1 protein kinase. *Proc. Natl. Acad. Sci. USA* 110, 17432–17437.
- Swinnen, E., Wanke, V., Roosen, J., Smets, B., Dubouloz, F., Pedruzzi, I., Camerini, E., De Virgilio, C., and Winderickx, J. (2006). Rim15 and the crossroads of nutrient signalling pathways in *Saccharomyces cerevisiae*. *Cell Div.* 1, 3.
- Traoré, D.A.K., El Ghazouani, A., Jacquamet, L., Borel, F., Ferrer, J.-L., Lascoux, D., Ravanat, J.-L., Jaquinod, M., Blondin, G., Caux-Thang, C., et al. (2009). Structural and functional characterization of 2-oxo-histidine in oxidized PerR protein. *Nat. Chem. Biol.* 5, 53–59.
- Treitel, M.A., Kuchin, S., and Carlson, M. (1998). Snf1 protein kinase regulates phosphorylation of the Mig1 repressor in *Saccharomyces cerevisiae*. *Mol. Cell Biol.* 18, 6273–6280.
- van Leemputte, F., Vanthienen, W., Wijnants, S., van Zeebroeck, G., and Thevelein, J.M. (2020). Aberrant intracellular pH regulation limiting Glyceraldehyde-3-phosphate dehydrogenase activity in the glucose-sensitive yeast tps1Δ mutant. *mBio* 11, e02199-20.
- Vercoulen, Y., Kondo, Y., Iwig, J.S., Janssen, A.B., White, K.A., Amini, M., Barber, D.L., Kuriyan, J., and Roose, J.P. (2017). A Histidine pH sensor regulates activation of the Ras-specific guanine nucleotide exchange factor RasGRP1. *Elife* 6, e29002.
- Vincent, O., Townley, R., Kuchin, S., and Carlson, M. (2001). Subcellular localization of the Snf1 kinase is regulated by specific beta subunits and a novel glucose signaling mechanism. *Genes Dev.* 15, 1104–1114.
- Wilson, W.A., Hawley, S.A., and Hardie, D.G. (1996). Glucose repression/derepression in budding yeast: SNF1 protein kinase is activated by phosphorylation under derepressing conditions, and this correlates with a high AMP:ATP ratio. *Curr. Biol.* 6, 1426–1434.
- Woods, A., Munday, M.R., Scott, J., Yang, X., Carlson, M., and Carling, D. (1994). Yeast SNF1 is functionally related to mammalian AMP-activated protein kinase and regulates acetyl-CoA carboxylase in vivo. *J. Biol. Chem.* 269, 19509–19515.
- Ye, T., Bendrioua, L., Carmena, D., Garcia-Salcedo, R., Dahl, P., Carling, D., and Hohmann, S. (2014). The mammalian AMP-activated protein kinase complex mediates glucose regulation of gene expression in the yeast *Saccharomyces cerevisiae*. *FEBS Lett.* 588, 2070–2077.
- Young, B.P., Shin, J.J.H., Orij, R., Chao, J.T., Li, S.C., Guan, X.L., Khong, A., Jan, E., Wenk, M.R., Prinz, W.A., et al. (2010). Phosphatidic acid is a pH biosensor that links membrane biogenesis to metabolism. *Science (New York, N.Y.)* 329, 1085–1088.
- Zahn, R. (2003). The octapeptide repeats in mammalian prion protein constitute a pH-dependent folding and aggregation site. *J. Mol. Biol.* 334, 477–488.
- Zhao, P., Zhao, C., Chen, D., Yun, C., Li, H., and Bai, L. (2021). Structure and activation mechanism of the hexameric plasma membrane H⁺-ATPase. *Nat. Commun.* 12, 6439.
- Zhao, Q., Li, C., and Li, S.J. (2015). The pH-sensitive structure of the C-terminal domain of voltage-gated proton channel and the thermodynamic characteristics of Zn²⁺ binding to this domain. *Biochem. Biophys. Res. Commun.* 456, 207–212.
- Zhou, H., and Winston, F. (2001). NRG1 is required for glucose repression of the SUC2 and GAL genes of *Saccharomyces cerevisiae*. *BMC Genet.* 2, 5.

STAR★METHODS

KEY RESOURCES TABLE

REAGENT or RESOURCE	SOURCE	IDENTIFIER
Antibodies		
Rabbit anti-GFP	Abcam	AB290 RRID: Ab_303395
Rabbit anti-phospho T172 (AMPK)	Cell Signalling Technologies	#2535 RRID: Ab_331250
Mouse anti-HA	Santa Cruz	F-7 RRID: Ab_2894930
Mouse anti-Pgk1	Abcam	Ab113687 RRID:Ab_10861977
Goat anti-mouse HRP	Jackson	115035003 RRID: Ab_10015289
Goat anti-rabbit HRP	Jackson	111035144 RRID: Ab_2307391
Bacterial and virus strains		
DH5 α	Lab Stock	N/A
Chemicals, peptides, and recombinant proteins		
2-Nitrophenyl - beta-D-galactopyranoside (ONPG)	Sigma	N1127
Y-PER	Thermo Scientific	#78990
2-mercaptoethanol	Fluka	M6250
Polynucleotide kinase	Sigma	PNK-RO
Ebselen	Sigma	E3520
Na ₂ CO ₃	Sigma	791768
Deposited data		
N/A		
Experimental models: Organisms/strains		
Please see Table 1		
Oligonucleotides		
Please see Table 3		
Recombinant DNA		
Please see Table 2		
Software and algorithms		
Image J	Image J	N/A
Graphpad	Graphpad: https://www.graphpad.com/quickcalcs/ttest1/?format=SD	N/A

RESOURCE AVAILABILITY

Lead contact

Further information and requests for strains and plasmids should be directed to and will be fulfilled by the lead contact Martin Kupiec (martin.kupiec@gmail.com).

Materials availability

All materials generated in this study are available on request to the [lead contact](#).

Data and code availability

Data reported in this article will be shared by the [lead contact](#) on request. This article does not report original code. Any additional information required to reanalyze the data reported in this article is available from the [lead contact](#) on request.

EXPERIMENTAL MODEL AND SUBJECT DETAILS

Yeasts, plasmids, and growth conditions

Experiments were conducted using *S. cerevisiae*. DH5a bacteria were used for plasmid propagation and standard procedures. Strains used are listed in Table 1; plasmids used are listed in Table 2. Oligonucleotide used for mutagenesis of Snf1 and Pma1 are listed in Table 3. All strains are related to W303a except for PJ694 used for yeast 2-hybrid assays. Yeasts were transformed with DNA using the frozen lithium acetate method (Knop et al., 1999). Construction of poly-amino acid substitutions in Snf1; and exchange of selective markers in plasmids was by gap repair (Ma et al., 1987) and PCR.

PMA1 (from -934 of promoter to +834 of 3'UTR) was inserted into the multiple cloning site of pRS313 and pRS314. The final 18 codons were truncated using Phusion PCR. Four or eight histidines were inserted into plasmid 847 using Phusion PCR. Primers were phosphorylated before use with polynucleotide kinase.

Standard sugar concentrations were 4% for glucose (to ensure complete repression of the *ADH2* promoter), 3% for glycerol and 2% for ethanol, unless stated differently. For *ADH2*, *ACS1*, and *JEN1* expression assays, cells were grown in 4% glucose to ensure complete repression of expression, washed 3x with water, and resuspended in media containing 2% ethanol. Cells were grown at 30°C.

METHOD DETAILS

β -galactosidase assays for gene expression

β -galactosidase assays were performed using log phase cells. Cells containing *prADH2/ACS1/JEN1::LacZ* plasmids were grown overnight in 4% glucose synthetic defined medium, diluted in the morning and grown for an additional 3 h. A sample was taken for measuring (t = 0) and cells washed 3x with 25 mL water before resuspension in indicated medium. After 3 h β -galactosidase activity was measured. Cell concentration was determined by reading 100 μ L of cells at 595 nm. 20 μ L of cells was added to the β -galactosidase reaction mix (40 μ L YPER (Pierce 78,990), 80 μ L Z-buffer (120 mM Na₂HPO₄, 80 mM NaH₂PO₄, 20 mM KCl, 2 mM MgSO₄), 24 μ L ONPG (4 mg/mL), 0.4 μ L β -mercaptoethanol) and incubated at 30°C for 15 min. Reactions were stopped by addition of 54 μ L 1 M Na₂CO₃. The Eppendorf tubes were centrifuged for 1 min at full speed to pellet the cell debris, and 200 μ L supernatant was removed, and absorbance read at 415 nm using a microplate reader. Miller Units were calculated by the equation Miller Units = (1000 * A₄₁₅) / (time * volume of cells * A₅₉₅ - 0.055), where the A₄₁₅ and A₅₉₅ has been corrected for blanking and path length (final path length = 1 cm). The expression was calculated as a rate of Miller unit increase per hour, and shown as a percentage of the expression rate of WT cells (=100). Typically, in wild-type cells, *ADH2* is expressed at 1000 Miller Units per hour in ethanol medium and barely expressed in glucose medium, *ACS1* at 1500 Miller Units/hour and *JEN1* at 1350 Miller Units/hour in ethanol medium. Three biological replicates were measured. Error bars are + - 1 standard deviation.

Yeast 2-hybrid experiments

S. cerevisiae strain PJ694 (*trp1-901 leu2-3,112, ura3-52, his3 Δ 200, gal4 Δ , gal80 Δ , prGAL2:ADE2 lys2::prGAL1::HIS3 met2::prGAL7-LacZ*) or PJ694 *hsp30 Δ* was transformed with the indicated plasmids expressing proteins or protein fragments fused to either GAD or GBD and PMA1- Δ 901 where indicated. Cells were grown overnight in indicated medium and diluted in the morning with the same medium for an additional 3 h before β -galactosidase activity was determined as above. However, for Figure 4F cells were grown in 2% ethanol overnight. After measuring t = 0 glucose to 2% and the indicated concentration of ebselen (in DMSO, from Sigma) was added and cells grown for an additional 4 h before the interaction between the NTD and CTD was determined. Three biological replicates were measured. Error bars are + - 1 standard deviation.

Western blots

For Figures 2E, 2G, and 4B, cells were grown overnight in 4% glucose, diluted in the morning and grown for an additional 3 h. A sample was taken, and the remaining cells washed 2x with 25 mL water and resuspended in 2% ethanol medium for the time indicated (minutes). For Figure 2G (a time-course) because centrifugation activates Snf1 (Orlova et al., 2008) a sample was taken in glucose grown cells (Glc), immediately after washing and resuspension in media containing 2% ethanol (0) and thereafter at indicated times. For Figures 2F and 4E glucose was added to ethanol grown cells to 2%. For Figure 4D, cells were grown in

2% ethanol medium overnight. After harvesting a sample (ethanol) glucose to 2% (+DMSO) and ebselen at the indicated concentrations (in DMSO) was added. Cells were harvested after 15 min.

Cells were harvested and protein solubilized in sample buffer by the method developed by the Kuchin group to prevent activation of Snf1 by centrifugation (Orlova et al., 2008). Cells were boiled for 5 min before resuspension in 1x TE and treatment with 0.2 M NaOH. Sample buffer volume was adjusted to give equal OD for all samples (30 μ L/OD) and cells boiled for 5 min. After running samples on 8% polyacrylamide gels, the proteins were wet transferred to nitrocellulose membranes. Antibodies used were mouse α -pgk1 (Abcam) for a loading control, rabbit α -GFP (Abcam), mouse α -HA (Santa Cruz) and rabbit α -phospho-T172 (AMPK) (Cell Signalling Technology), all at 1/1000 dilution. Because Snf1-GFP and Rod1-6HA run at 100 kDa, the membrane was cut between 55 and 65 kDa (to check at 72 kDa if native Snf1 is present – it was absent from all samples), the lower half used for Pgk1 and the upper for HA, GFP or phospho-T172. Secondary antibodies were conjugated to HRP. Images were minimally processed using ImageJ.

Microscopy

snf1 Δ ADE2 cells carrying *prSNF1::Snf1-GFP* plasmids with the indicated mutations [deletion of polyHIS (Δ H), substitution to poly^A (A), poly^F (F), poly^K (K), poly^W (W), poly^Y (Y), T210A] were grown overnight in medium containing 4% glucose. 1 mL of cells were washed 3x with water, and resuspended in medium containing 3% glycerol for 30 min. 5 μ L of log phase cells were imaged using an EVOS microscope (60x objective) with the GFP filter for GFP and the Texas Red filter for Cherry. The dimension of each panel corresponds to 20 \times 20 μ m. Cells were not concentrated before imaging, to prevent perturbations to Snf1 activity (Wilson et al., 1996). Images were processed using the brightness/contrast function of Image J, to give a black background. For statistics, over 300 cells were counted. Experiments were repeated at least three times on different days. All figures shown in the manuscript are of identical magnification, a size bar is provided in Figure 2C.

Serial dilutions

snf1 Δ cells were transformed with centromeric plasmids expressing *prSNF1::SNF1-GFP* with the indicated mutations (deletion of polyHIS (Δ H), substitution to poly^A (A), poly^F (F), poly^W (W), poly^Y (Y)) or empty vector, and *snf1 Δ mig1 Δ* cells were transformed with empty vector. Cells were grown in medium lacking leucine with 4% glucose overnight, washed 3x with water and resuspended in water at a concentration of 7.5OD⁶⁰⁰/mL. Cells were serially diluted 10-fold and spotted onto-Leu plates with either 2% glucose, 2% galactose, or 3% glycerol as the carbon source and incubated at 30°C for 2 days. Cells were imaged using a Samsung A50 camera.

QUANTIFICATION AND STATISTICAL ANALYSIS

Data were analyzed using a two-tailed unpaired t-test (GraphPad). Unless indicated, data points were compared to the strain/condition designated as 100%. * = p0.05, ** = p0.01, *** = p0.001, NS = Not significant.